and sagittal sections. The entire animals were sectioned and every section examined. Selective labeling was found exclusively in the calceoli (Fig. 1). The calceoli are extremely thin and fragile, and many of them were torn or completely lost in histological processing. The remaining ones, however, were very distinctly labeled. In several instances, labeling could be traced in different parts of the same calceolus in two or three consecutive sections.

It was concluded that the females produce a compound, apparently a sex pheromone, which acts over a distance in the water and agitates and attracts the males. The experiments prove that the calceoli on the male second antenna contain the receptors for this stimulus.

ERIK DAHL, HADAR EMANUELSSON
CLAES VON MECKLENBURG
Departments of Zoology and
Zoophysiology, University of Lund, Lund, Sweden

16 February 1970; revised 31 July 1970

Secondary Structure of Ribosomal RNA

Abstract. *Infrared spectra were obtained for 16S and for 23S ribosomal RNA's in D_2O solutions. The percentage of each base in the paired and unpaired regions of the RNA was determined from the spectra. The secondary structures of 16S and 23S ribosomal RNA's (from* Escherichia coli*) are significantly different from each other and are also different from those of yeast ribosomal RNA, formylmethionyl–transfer RNA, and the anticodon fragment of this transfer RNA.*

The secondary structure of ribosomal RNA (rRNA) in the ribosome is considered to be similar to that of protein-free rRNA (*1*), which consists of single-stranded regions (with no hydrogen bonds between bases) alternating with helical, double-stranded regions with hydrogen bonds between bases (*1*, *2*). These hydrogen bonds perturb vibrational modes and thus alter the infrared spectra of the bases. This effect has been used in a new method that gives the percentage of RNA bases in the double-stranded and single-stranded regions and the average base composition of these regions (*3*). This method has been applied to unfractionated rRNA from yeast (*3*) and from *Escherichia coli* (*4*), to crystallizable fragments of yeast rRNA (*2*), to a transfer RNA (tRNA) (*5*), and to anticodon fragment of a tRNA (*6*).

Table 1. Percentage of rRNA bases in paired and unpaired states at 26°C. The base composition (*1*) of 16*S* rRNA is (in percent) 24.5 A, 21.5 U, 31.5 G, and 22.5 C; that of 23*S* rRNA is 25.5 A, 20.7 U, 32.8 G, and 21.0 C.

Bases	16*S* rRNA	23*S* rRNA
A + U paired	24.0	25.0
G + C paired	36.0	33.0
A unpaired	12.5	13.0
U unpaired	9.5	8.2
G unpaired	13.5	16.3
C unpaired	4.5	4.5

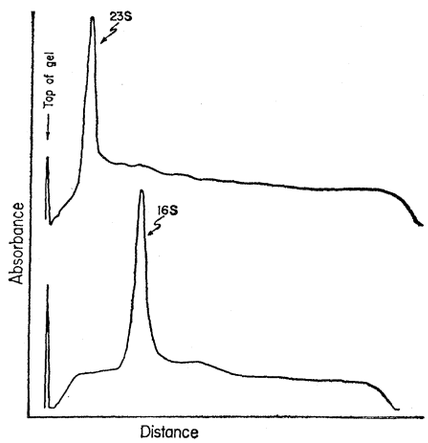

Fig. 1. Polyacrylamide-gel electrophoresis of 23*S* rRNA (upper curve) and 16*S* rRNA (lower curve) recovered from the infrared cell after spectra were recorded.

We measured the infrared spectra of purified 23*S* and 16*S* rRNA's from *E. coli*. Analysis shows that small but significant differences exist in the secondary structures of these two species.

The 16*S* and 23*S* rRNA's were extracted by the sodium dodecyl sulfate (SDS)–phenol method from 30*S* and 50*S* ribosomes isolated from *E. coli* D10 (*7*). After the ether treatment, the alcohol precipitation step was repeated three times to ensure that all phenol was removed from the RNA. After the final precipitation, the alcohol solution was removed from the pelleted RNA, which was dried with a flow of dry air to a hard transparent solid.

To obtain infrared spectra, dried RNA was dissolved to a concentration of 40 mg/ml in D_2O (99.8 percent; Diaprep Inc.) containing 0.1 percent SDS. No buffers were used because RNA is self-buffering at these concentrations (*2*, *3*). The *p*D of the solutions was 7.2 ± 0.4. Dust and air bubbles were removed from the RNA solutions by centrifugation at 6000*g*. The total concentration of RNA bases in the solution was determined by measuring the ultraviolet spectrum of a portion of the RNA solution which had been hydrolyzed with NaOH (*2*). Infrared spectra were obtained in a thermostated cell with path length of 75 μm. A reference cell was used to compensate for the absorbance of the D_2O (*2*).

The integrity of the RNA in the solutions recovered from the infrared cell was determined by electrophoresis on 3.75 percent polyacrylamide gels (*7*). The gels were scanned for absorbance at 2600 Å with a Gilford spectrophotometer and scanning attachment. The electrophoretograms of both 16*S* and 23*S* rRNA's recovered from the infrared cell showed one large band at the correct location with only slight amounts of lower molecular weight material and were quite similar to the electrophoretograms of the input samples (Fig. 1). We conclude that no significant amount of degradation occurred while the spectra were recorded.

To obtain quantitative estimates of the secondary structure of RNA, we

Table 2. Base composition (mole percent) of the paired and unpaired regions of rRNA's.

Base	16*S* rRNA	23*S* rRNA
A paired	21.5	20.0
U paired	21.5	20.0
G paired	28.5	30.0
C paired	28.5	30.0
A unpaired	31.0	31.2
U unpaired	19.5	23.8
G unpaired	38.8	33.8
C unpaired	10.7	11.2

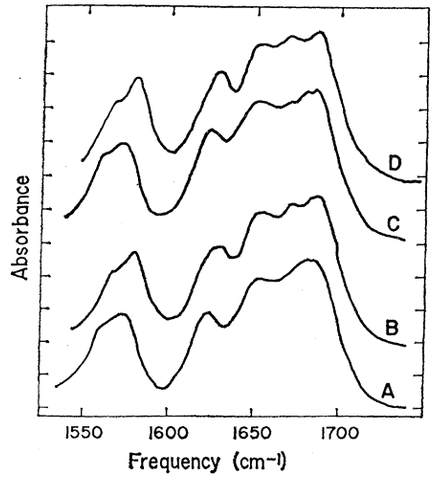

Fig. 2. Infrared spectra of 16*S* and 23*S* rRNA's. (A) Observed spectrum of 16*S* rRNA; (B) synthesized spectrum of 16*S* rRNA; (C) observed spectrum of 23*S* rRNA; and (D) synthesized spectrum of 23*S* rRNA.

have synthesized spectra, which give a best fit to the observed spectra, by summing the individual spectra for adenine–uridine (AU) and guanine–cytosine (GC) base pairs and for unpaired A, U, C, and G (*8*). Therefore we have assumed that only Crick-Watson base pairs exist. The observed and synthetic spectra for 16*S* and 23*S* rRNA's (Fig. 2) are in close agreement. An exact fit is not expected since perturbations in the spectra of those unpaired bases in stacked configurations are neglected in this method (*2*). The percentage of each species used to obtain the best-fit synthesis is interpreted as the percentage of that species occurring in the RNA (Table 1). The base composition of the base-paired and unpaired regions of the RNA was calculated from Table 1 and is shown in Table 2.

These data are useful in comparing the secondary structures of 16*S* and 23*S* rRNA's rather than as an absolute measure of structure (*9*). The 16*S* and 23*S* rRNA's from *E. coli* have similar amounts of AU and GC base pairs in their secondary structures (Table 1). At 26°C, both 16*S* and 23*S* rRNA's have about 60 percent of their bases in paired regions and contain appreciably more GC than AU pairs (*10*). These *E. coli* rRNA's exhibit less base pairing than yeast rRNA (which is 64 percent paired at 30°C) but have a similar percent of GC pairs and less AU pairs (*2*). In contrast, 72 percent of the bases of formylmethionyl tRNA are paired, but only 32 percent of the bases of the anticodon fragment of this tRNA are paired (*5, 6*). It is clear that differences in base sequence between these species of RNA cause significant differences in secondary structure.

The data also show that significant differences exist in the secondary structures of 16*S* and 23*S* rRNA's from *E. coli*. Thus 16*S* has more total pairing and more GC and less AU pairs than does 23*S*. We may expect that some of the paired regions of 16*S* will have a greater stability than those of 23*S*. The 16*S* rRNA may also have larger continuous regions of pairing because regions with higher GC content would have sufficient stabilization energy to accommodate more base mispairing of the Wobble type (*11*) than would regions of low GC content. The single-stranded nonpaired regions of 16*S* rRNA contain more G than do similar regions in 23*S* (39 versus 34 percent) (Table 2). We may therefore expect a larger stacking interaction in the nonpaired regions of 16*S* than in 23*S*, which may mean that 23*S* rRNA is more flexible than 16*S* rRNA. Differences in secondary structure will determine differences in tertiary structure. Because the single-stranded regions of both 16*S* and 23*S* rRNA's from *E. coli* have a similar percent of pyrimidines, it might be expected that the rates of hydrolysis of these species by ribonuclease A would be similar. The fact that the rates are different (*7*) indicates that differences in tertiary structure may well exist as suggested by the data presented here.

K. A. HARTMAN
Department of Bacteriology and Biophysics, University of Rhode Island, Kingston 02881

G. J. THOMAS, JR.
Department of Chemistry, Southeastern Massachusetts University, North Dartmouth 02747

References and Notes

1. A. S. Spirin and L. P. Gavrilova, *The Ribosome* (Springer-Verlag, New York, 1969).
2. G. J. Thomas, Jr., and M. Spencer, *Biochim. Biophys. Acta* **179**, 360 (1969).
3. G. J. Thomas, Jr., *Biopolymers* **7**, 325 (1969).
4. R. I. Cotter and W. B. Gratzer, *Nature* **221**, 154 (1969).
5. M. Tsuboi, S. Higuchi, Y. Kyogoku, S. Nishimura, *Biochim. Biophys. Acta* **195**, 23 (1969).
6. K. Morikawa, M. Tsuboi, Y. Kyogoku, T. Seno, S. Nishimura, *Nature* **223**, 537 (1969).
7. K. A. Hartman, J. Amaya, E. M. Schachter, *Science* **170**, 171 (1970).
8. The component spectra were obtained by using the spectrum of poly(A · U) for AU, poly-(G · C) for GC, and the respective 5′-nucleotides for unpaired A, U, G, and C.
9. The sensitivity of the values in Table 1 is ± 1 percent, whereas the accuracy may be as low as ± 10 percent. Therefore comparison within Table 1 is meaningful, even though systematic error may exist for all values.
10. These results are consistent with those obtained in (*4*) for unfractionated *Escherichia coli* rRNA.
11. F. H. C. Crick, *J. Mol. Biol.* **19**, 548 (1966).
12. This work was supported by grant GB 8150 from the National Science Foundation and by the Department of Chemistry, Southeastern Massachusetts University.

20 August 1970

Climatic Anomaly over the United States during the 1960's

Abstract. *The past cool decade over the eastern United States is attributed to increased deployment of polar air masses set in motion by responses of the upper-air wind circulation of the Northern Hemisphere to large-scale air-sea coupling over the North Pacific.*

Climatic fluctuations on all time scales have always received a great deal of attention, and the cooling trend observed in numerous areas of the world during the 1960's has been no exception (*1*). Speculation as to the cause of the cooling has involved air pollution, volcanic activity, solar variations, and other more bizarre phenomena. Generally omitted from consideration is large-scale and long-term air-sea interaction—perhaps because of the unavailability of reliable long series of oceanic temperature data or because of

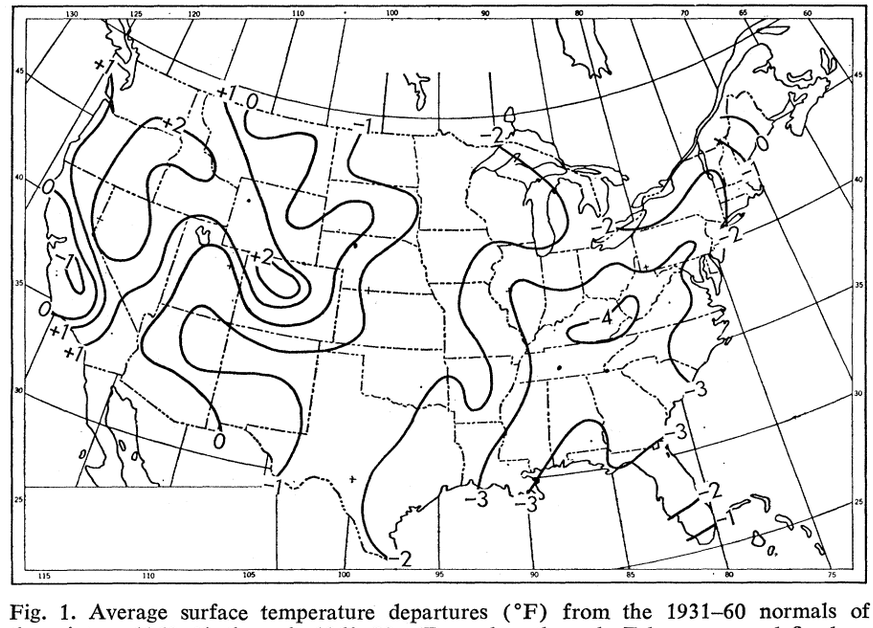

Fig. 1. Average surface temperature departures (°F) from the 1931–60 normals of the winters 1960–61 through 1969–70. (December through February are defined as the winter months.)